sustainability

MDPI

Article

Multi-Objective Optimization of the Structural Design of a Combustion Chamber of a Small Agricultural Diesel Engine Fueled with B20 Blend Fuel at a High Altitude Area

Zhipeng Shi [1,2], Jun Wang [1,2,*], Xiangchi Guo [1,2] and Xueyuan Liu [1,2]

1 School of Mechanical and Transportation, Southwest Forestry University, Kunming 650224, China; 18512559766@163.com (Z.S.); guoxiangchi2021@163.com (X.G.); lxy98t@126.com (X.L.)

2 Key Laboratory of Vehicle Emission and Safety on Plateau Mountain, Yunnan Provincial Department of Education, Kunming 650224, China

* Correspondence: zjwj1121@163.com

Abstract: This study focuses on a small agricultural diesel engine fueled with B20 (20% biodiesel and 80% diesel by volume) blend fuel in a plateau area. The combustion chamber's structural parameters and fuel injection angle were taken as variables at peak torque conditions. First, a full factorial design was used for experimental design. Second, the back-propagation (BP) neural network was employed to predict the indicated thermal efficiency and the indicated specific NO_x emission. Third, the non-dominated sorting genetic algorithm-II (NSGA-II) was utilized to optimize the indicated thermal efficiency and the indicated specific NO_x emission. Finally, the technique for order of preference by similarity to ideal solution (TOPSIS) method was applied to obtain optimal solutions, and a three-dimensional numerical simulation was conducted to verify the optimization results. The optimization results indicate that the shape characteristics of the combustion chamber have a certain influence on the engine's performance. The optimized design significantly reduces NO_x emissions, by 22.83%, compared to the original engine, whilst maintaining the engine's performance.

Keywords: agricultural diesel engine; combustion chamber; biodiesel; multi-objective optimization; altitude

Citation: Shi, Z.; Wang, J.; Guo, X.; Liu, X. Multi-Objective Optimization of the Structural Design of a Combustion Chamber of a Small Agricultural Diesel Engine Fueled with B20 Blend Fuel at a High Altitude Area. *Sustainability* **2023**, *15*, 11617. https://doi.org/10.3390/su151511617

Academic Editor: Zafar Said

Received: 12 May 2023
Revised: 19 July 2023
Accepted: 25 July 2023
Published: 27 July 2023

1. Introduction

In recent years, China's agricultural mechanization has rapidly developed, and the output of agricultural machinery consistently ranks first in the world [1]. Over 95% of agricultural machinery utilizes diesel engines as power units [2,3], with their diesel consumption accounting for approximately one-third of the nation's total diesel consumption. Because carbon dioxide (CO_2) emissions from internal combustion engines are directly proportional to fuel consumption, agricultural machinery is one of the major sources of carbon emissions. However, due to their long-term operation under low-speed and high-load conditions [4], their operation in complex and diverse environments, and their wide range, agricultural machinery has been found to emit substantial amounts of pollutants, while their emission control technology remains relatively outdated [5]. In 2021, China's agricultural machinery emitted 205,000 tons of hydrocarbons (HC), 1.671 million tons of nitrogen oxides (NO_x), and 92,000 tons of particulate matter (PM). Among the non-road mobile sources, agricultural machinery accounted for 47.8% of HC emissions, 34.9% of NO_x emissions, and 39.3% of PM emissions [6], highlighting the significant contribution of agricultural machinery to pollution emissions.

China possesses a wide distribution of plateaus and mountains, with plateaus above 1000 m covering approximately 58% of the country's total area, and those above 2000 m accounting for 33% [6,7]. A large number of agricultural machinery powered by diesel engines operate in plateau areas where lower atmospheric pressure reduces fresh air flow into the cylinder, leading to compromised combustion, decreased thermal efficiency, power performance, and fuel economy, and increased emissions of carbon monoxide (CO), HC, and PM [8–10]. In the context of a low-carbon economy, particularly China's commitment to carbon peaking and carbon neutrality goals, internal combustion engines fueled with alternative fuels have garnered renewed attention. Among alternative fuels such as biodiesel, alcohols, ethers, natural gas, Fischer–Tropsch diesel, and ammonia [11], biodiesel is the most widely used and shows great potential as an alternative fuel for diesel engines [12,13]. Biodiesel, being a typical oxygenated fuel with a high cetane number, promotes more complete combustion [14,15], thereby helping to alleviate the issue of pollutant emissions caused by incomplete combustion in plateau environments.

The combustion chamber structure directly influences the fuel and air mixing process within the cylinder [16,17], playing a crucial role in diesel engine performance and emissions [18]. Lei et al. [19] discovered that an appropriate increase in the shrinkage ratio of the combustion chamber promotes turbulent motion within the cylinder, thereby enhancing the mixture quality and the combustion process. Taghavifar et al. [20] demonstrated that as the combustion chamber's concave radius (piston bowl radius) increases or the throat position decreases, NO_x emissions gradually increase, while soot emissions gradually decrease. Zheng et al. [21] demonstrated that optimizing the combustion chamber structure improves air flow motion within the cylinder, thereby accelerating the flame propagation rate and achieving better brake thermal efficiency. Guo et al. [22] proved that a relatively flat combustion chamber with a small lip depth and a moderate concave arc radius can result in a higher indicated thermal efficiency. Zhang et al. [23] optimized combustion chamber parameters, and bench tests indicated a reduction in weighted fuel consumption by 2.2 g/(kW·h) during the European steady-state cycle with the optimized combustion chamber, while the weighted NO_x emission remained almost the same as the original one. Lee et al. [24] demonstrated that optimizing the combustion chamber and employing a compression ratio of 18 reduced fuel consumption by 1.5%, and the emissions from the diesel engine met the EU non-road Stage V emission standards. Liu et al. [25] achieved an 1.8% improvement in brake thermal efficiency by appropriately increasing the compression ratio and optimizing the combustion chamber parameters and nozzle angle; however, this also led to an increase in NO_x emissions.

The previous research primarily focused on improving the combustion chamber and injection parameters for diesel engines fueled with fossil diesel. However, biodiesel has different physicochemical properties from fossil diesel, resulting in variations in spray and combustion characteristics. Directly burning biodiesel–diesel mixed fuel or biodiesel in a diesel engine may not achieve optimal performance. Therefore, it is necessary to enhance the combustion chamber structure and fuel injection parameters of a diesel engine fueled with biodiesel–diesel mixed fuel or biodiesel to attain better combustion efficiency and lower emissions, adapting to the properties of biodiesel–diesel mixed fuel or biodiesel. Jaichandar et al. [26] demonstrated that the brake thermal efficiency of a toroidal combustion chamber was higher than that of hemispherical and shallow-depth combustion chambers when a single-cylinder diesel engine was fueled with 20% pongamia biodiesel. They also found that using a toroidal combustion chamber significantly reduced CO, HC, and smoke emissions, while NO_x emissions slightly increased. Furthermore, Jaichandar et al. [27] observed that compared to a baseline engine fueled with diesel, using a toroidal combustion chamber and retarding injection timing improved brake thermal efficiency by 5.64%, reduced fuel consumption by 4.6%, and increased NO_x emissions by 11.0% when the diesel engine was fueled with 20% pongamia biodiesel. Similar conclusions were drawn when a toroidal combustion chamber was combined with high fuel injection pressure [28]. Li et al. [29] indicated that among three types of combustion chambers (hemispherical, omega, and shallow-depth), a shallow-depth combustion chamber was conducive to improving the low-speed performance of a diesel engine fueled with biodiesel, while an omega combustion chamber was more suitable for high-speed conditions. However, both of them resulted in higher nitric oxide (NO) emissions at each operating condition. Premnath et al. [30] revealed that when a diesel engine equipped with a reentrant combustion chamber was fueled with 20% jatropha biodiesel, it experienced a 26% reduction in CO emissions, a 24% reduction in HC emissions, and a 24% reduction in smoke emissions compared to when fueled with diesel. Bapu et al. [31] demonstrated that compared to a traditional hemispherical combustion chamber, a modified hemispherical combustion chamber significantly reduced CO, HC, and smoke emissions when used with 20% biodiesel in the diesel engine. Karthickeyan et al. [32] pointed out that when a diesel engine was fueled with biodiesel, a toroidal combustion chamber exhibited better engine performance compared to a hemispherical combustion chamber or a trapezoidal combustion chamber. Due to the oxygen content in biodiesel, CO, HC, and smoke emissions were reduced, except for NO_x, when compared to burning diesel. Khan et al. [33] reported that among the toroidal reentrant combustion chamber, reentrant combustion chamber, and hemispherical combustion chamber, the single-cylinder diesel engine fueled with soybean biodiesel combined with the reentrant combustion chamber, displayed advantages in terms of performance, combustion, and emissions. Shivashimpi et al. [34] claimed that when burning pongamia biodiesel with different blending ratios, the diesel engine equipped with modified cylindrical, shallow-depth, and toroidal combustion chambers all reduced NO_x emissions compared to the baseline hemispherical combustion chamber. Rajashekhar et al. [35] improved the brake thermal efficiency and reduced CO and HC emissions of the diesel engine fueled with jatropha biodiesel by modifying the combustion chamber structure and increasing the injection pressure. Based on the aforementioned studies, when a diesel engine is fueled with different types of biodiesel, brake thermal efficiency can be improved, and CO, HC, and smoke emissions can be reduced. Moreover, the increased NO_x emissions resulting from burning biodiesel can be mitigated by enhancing the combustion chamber structure and injection parameters.

However, the aforementioned studies were primarily conducted in plain areas. The working medium entering the cylinder differs in plateau areas due to the presence of thin air. Furthermore, existing studies on the performance, combustion, and emissions of diesel engines fueled with biodiesel in plateau areas have almost exclusively been carried out without modifying the combustion chamber structure [36–40]. Therefore, in this study, a small agricultural diesel engine fueled with B20 (20% biodiesel and 80% diesel by volume) blend fuel at an altitude of approximately 2000 m was chosen as the research object, and combustion chamber structural parameters and fuel injection angle were taken as variables at the peak torque conditions. The full factorial design was adopted to conduct experimental design, the BP neural network was used to predict the indicated thermal efficiency and indicated specific NO_x emission, the non-dominated sorting genetic algorithm-II (NSGA-II) was employed to optimize the indicated thermal efficiency and indicated specific NO_x emission, and the technique for order of preference by similarity to ideal solution (TOPSIS) was employed to obtain the optimal solutions. This research aims to provide guidance for achieving clean and highly efficient combustion of diesel engines fueled with biodiesel in plateau areas.

2. Numerical Methodology

2.1. Establishment of the Numerical Model

The main parameters of the engine are presented in Table 1, featuring a deep pit ω-type combustion chamber. The engine is an inline four-cylinder, four-stroke turbocharged diesel engine. The injectors are equipped with six spray holes, each with a bore diameter of 0.122 mm and an oil beam angle of 156°.

Table 1. Engine specifications.

Parameter	Value
Bore × stroke	80 mm × 92 mm
Displacement	1.85 L
Compression ratio	16.5
Rated power	58 kW at 2500 r/min
Peak torque	265 N·m at 1800 r/min

The CFD software AVL-Fire 2020 R1 was used to import the surface model and construct the three-dimensional calculation model of the piston at top dead center (TDC), considering the relevant engine parameters. The model diagram can be seen in Figure 1. In this study, negative values of the crankshaft angle indicate the piston before top dead center (BTDC), while positive values indicate the piston after top dead center (ATDC). After verifying the mesh stability, an average mesh with a size of 0.0005 m was chosen, resulting in a total of 26,496 meshes. Because the operation of an internal combustion engine involves various reactions, several physical sub-models need to be employed. The selected sub-models for this study include the κ–ζ–f turbulence model [41], Dukowicz evaporation model [42], WAVE spray breakup model [43], Walljet 1 spray wall interaction model [44], ECFM-3Z extended coherent flame model [45], and the Heywood + temperature fluctuations model [46].

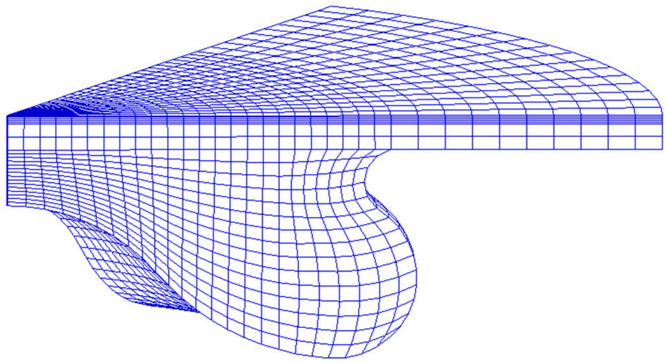

Figure 1. One-sixth grid model of the combustion chamber.

The fuel mechanism used in this study is a three-component skeletal reaction mechanism consisting of methyl decanoate, methyl 9-decanoate and n-heptane for the combustion of biodiesel in diesel engines. It contains 112 substances involved in 498 reactions, encompassing CO, NO_x, and soot formation mechanisms. The mechanisms are applicable in simulating diesel engine combustion fueled by biodiesel, diesel, and their blends [47].

This study uses a biodiesel–diesel blend as the fuel, requiring knowledge of the physical properties of the fuel for simulation purposes. A comparison of the physical properties between diesel fuel and biodiesel is presented in Table 2. Ambarish et al. [48] indicated that 20% biodiesel has the highest thermal efficiency, lowest fuel consumption, and lower emissions. Therefore, only B20 (20% biodiesel and 80% diesel by volume) was selected for this study, as supported by refs [26,27,30,31].

Table 2. Comparison of physical properties of fuels.

Parameters	Diesel	Biodiesel
Low calorific value	42.65 MJ/kg	38.56 MJ/kg
Hexadecane value	53.1	56.1
Density at 15 °C	843.6 kg/m^{-3}	875.9 kg/m^{-3}
Viscosity at 40 °C	2.72 mm^2/s	4.29 mm^2/s
Oxygen mass fraction	0.0%	10.0%

2.2. Model Validation

The engine was tested at an altitude of 2000 m, with an average atmospheric pressure of 0.8 bar, and the peak torque condition (1800 r/min full load) was chosen as the research condition. The selected computational model was initialized with the appropriate boundary conditions. The simulated in-cylinder pressure and heat release rate of B20 were compared to the experimental results, as shown in Figure 2. The simulated results closely match the experimental results for both the cylinder pressure and heat release rate plots. In the cylinder pressure graph, the peak cylinder pressure in the test occurs at around 9 °CA with a value of 13.67 MPa, while in the simulated work graph, the peak cylinder pressure is also at around 9 °CA with a value of 13.68 MPa. Additionally, both the simulated and test results show that the heat release rate starts to rise to around −9 °CA and peaks at around 7 °CA. Figure 3 illustrates the comparison of the indicated thermal efficiency and the indicated specific NO_x emission between the simulation and the test. The error between the simulated and tested data is limited to 5%, indicating that the established model accurately captures the actual operating trends.

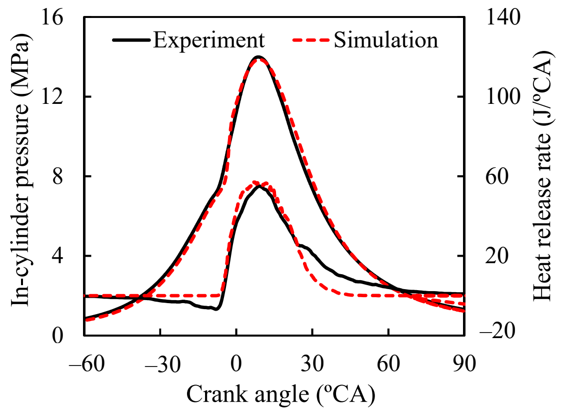

Figure 2. Comparison of in-cylinder pressure and heat release rate for B20 between the experiment value and simulation value.

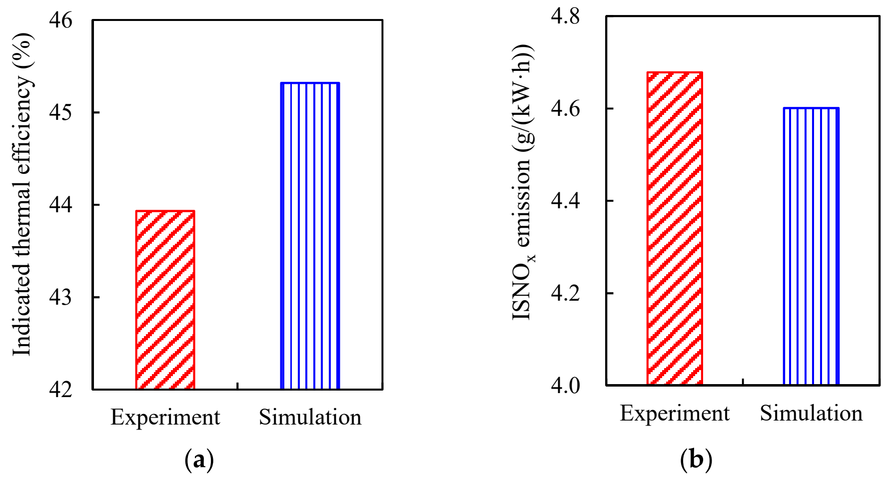

Figure 3. Comparison of indicated thermal efficiency and indicated specific NO_x emission for B20 between the experiment value and simulation value. (**a**) Indicated thermal efficiency. (**b**) Indicated specific NO_x emission.

3. Research Results and Analysis

3.1. Selection of Combustion Chamber Characteristics

The combustion chamber of a diesel engine exhibits various shape characteristics, and it is crucial to identify the influential characteristic parameters to optimize the engine's power and NO_x emissions. For this test, three commonly selected characteristic parameters are crater radius (r_1), center depth (h_1), and radius of throat opening (r_2) combined with the injection cone angle (α). The variations in the shape characteristics of the combustion chamber are depicted in Figure 4. The specific combustion chamber employed in this study is a deep pit ω-type combustion chamber, and the combustion chamber structure parameters are selected within the maximum range while maintaining this specific type of combustion chamber. Additionally, each scheme is modified according to the rules of CFD software to ensure a constant compression ratio by adjusting the head clearance of the combustion chamber.

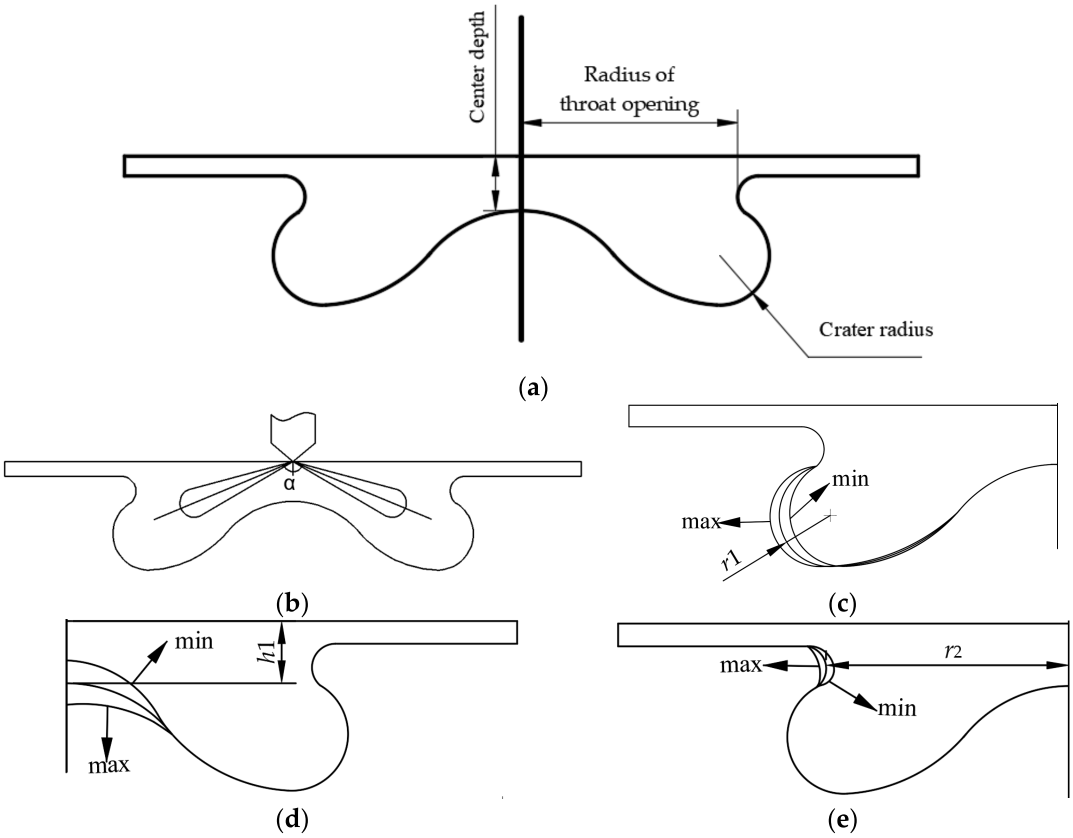

Figure 4. Schematic of diesel engine combustion chamber characteristic parameters. (**a**) Combustion chamber characteristics. (**b**) Injection cone angle α. (**c**) Crater radius r_1. (**d**) Center depth h_1. (**e**) Radius of throat opening r_2.

3.2. Experiment Design

To achieve the optimization goal, it is necessary to start with the experimental design, establish a regression model based on the simulation results from the established 3D diesel engine combustion chamber model, validate the model's validity, and ultimately determine the optimal combination of combustion chamber characteristic parameters and fuel injection parameters using an algorithm.

Due to the varying effects of the combustion chamber's characteristics on the combustion and emission performance of the diesel engine, several parameters with the maximum influence are selected as the factors. Considering the number of factors and response variables that are to be explored, a full factorial design method is chosen for the test to reduce the number of tests and improve the results. This means that combinations of all levels of factors are tested at least once. Specifically, for the operation of off-road diesel engines burning B20 biodiesel in the 2000 m area, four main calibration parameters were selected: combustion chamber center depth, crater radius, throat radius, and injection cone angle of the nozzle. These parameters are analyzed with three levels, and the range of values for each factor is presented in Table 3.

Table 3. Experimental design factor level for each combustion chamber characteristics at 2000 m.

Level	Injection Cone Angle α (°)	Crater Radius r_1 (mm)	Center Depth h (mm)	Throat Radius r_2 (mm)
−1	153	4.0	4.0	20.5
0	156	5.0	5.5	21.5
1	159	6.0	7.0	22.5

3.3. Model Building and Evaluation Based on BP Neural Network

Using the 81 sets of data acquired from the full analysis factor design, a BP neural network was employed to model and predict the impact of the selected factors on the indicated efficiency and the indicated NO_x emissions of the diesel engine after operation. It is worth noting that the accuracy of the BP neural network prediction results is influenced by the number of neuron nodes. For this study, 60 sets of samples were allocated to the training set, while 21 sets of samples were assigned to the test set. Through numerical simulation, the optimal number of neuron nodes was determined to be in the range of 7 to 15. The outcomes of the test are shown in Figure 5.

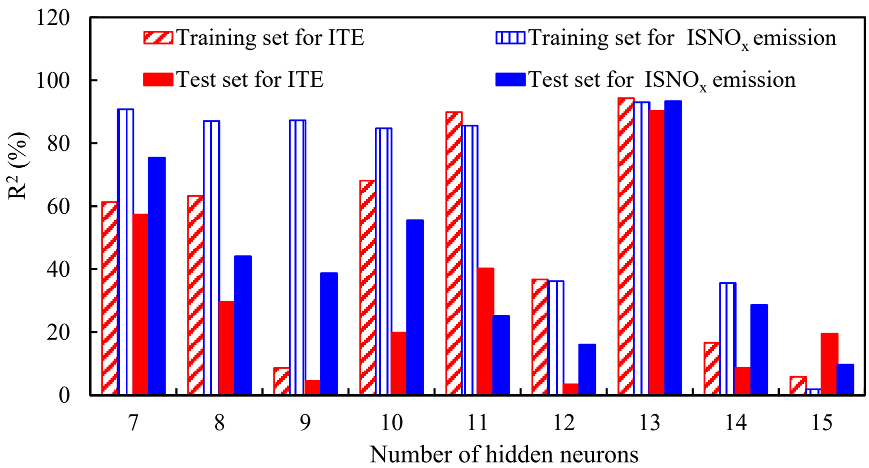

Figure 5. Effect of the number of hidden neurons on R^2.

Based on Figure 5, it is evident that the maximum variance R^2, greater than 90%, is achieved when the number of neuron nodes is set to 13. This indicates that the predictions for both the indicated efficiency and indicated NO_x emissions exhibit strong feasibility for the 60 sets of samples in the training set as well as the test set. As a result, the number of neuron nodes is selected as 13 for the subsequent model testing phase.

As depicted in Figure 6, the variance in the R^2 training set and R^2 test set for the BP neural network predicting the indicated thermal efficiency and indicated specific NO_x emission results exceeded 90%, with values of 94.32% and 93.03% for the former, and 93.31% and 90.26% for the latter, respectively. These high variances indicate that the model is capable of accurately predicting the actual results. With the model construction completed, the subsequent phase involves optimizing multiple objectives for multiple outcomes.

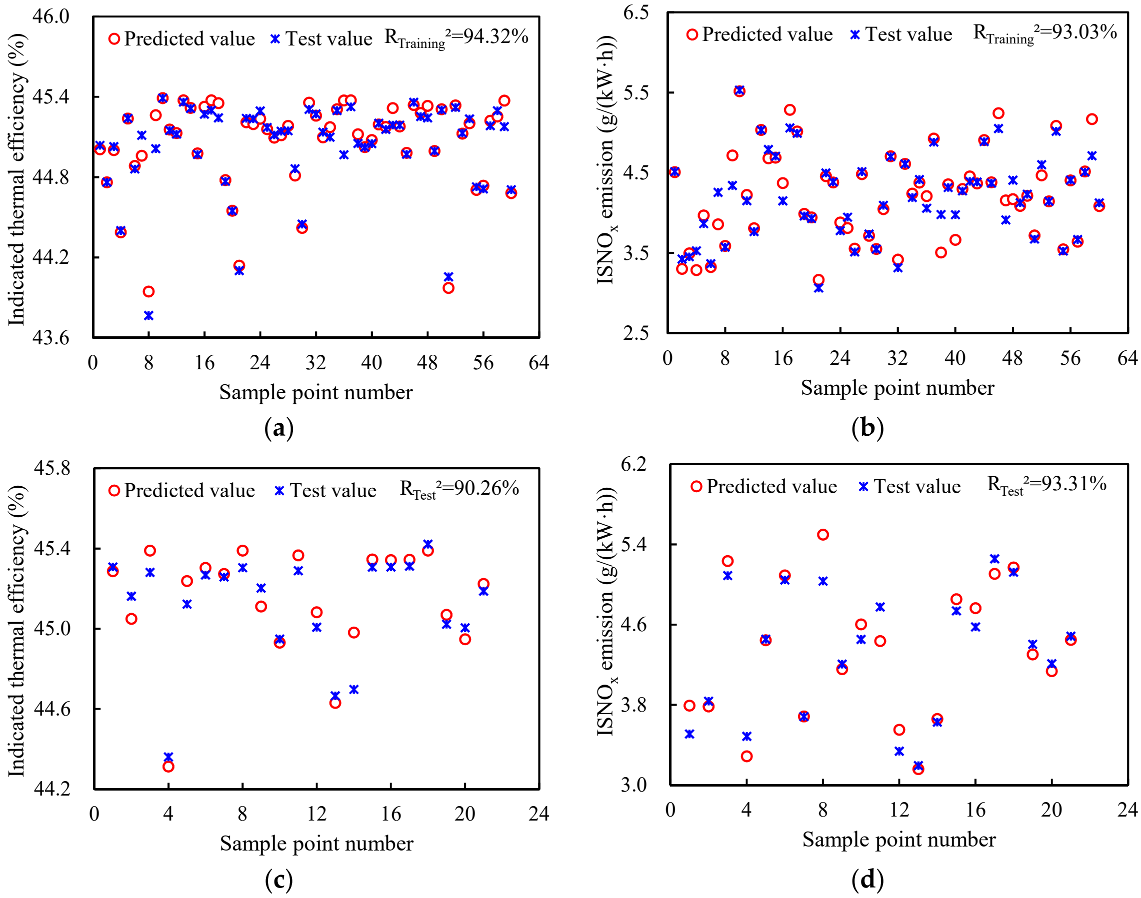

Figure 6. Prediction values of the BP neural network model. (**a**) Indicated thermal efficiency for training set. (**b**) ISNO$_x$ emission for training set. (**c**) Indicated thermal efficiency for test set. (**d**) ISNO$_x$ emission for test set.

3.4. Multi-Objective Optimization of Diesel Engine Dynamics and Emissions

To address the challenges of low-pressure and low-oxygen operating conditions, and considering the environmental and energy-saving aspects, it is feasible to use biodiesel as an alternative fuel for pure diesel fuel. However, this substitution leads to a significant increase in NO$_x$ emissions. Therefore, it is necessary to employ physical means to improve diesel engines and reduce NO$_x$ emissions when burning biodiesel in highland environments. A multi-objective optimization approach can help strike a better balance between indicated thermal efficiency and indicated specific NO$_x$ emission, considering both combustion and emission characteristics.

In this research, NSGA-II is used to optimize the combustion and emissions of small agricultural diesel engines. NSGA-II is a multi-objective optimization algorithm based on genetic algorithms. The algorithm begins by generating an initial population of size N through random selection, crossover, and mutation. In subsequent generations, the parent and child populations are combined, and non-dominated sorting and individual crowding are used to select suitable individuals for the new parent population based on non-dominated relationships and individual crowding. This process is repeated until the desired results are obtained.

To enable the optimization using NSGA-II, the corresponding objective functions need to be constructed. In this case, the preferred objective functions are to minimize the indicated specific NO$_x$ emissions and maximize the indicated thermal efficiency. Additionally, constraints are applied to prevent in-cylinder pressure and vortex front temperature from exceeding the fixed values during engine operation. For optimization purposes, the two selected objective functions are normalized, and the final results are represented using Equation (1).

$$
\begin{aligned}
& \mathit{min}\ \mathrm{ITE},\ \mathit{min}\ \mathrm{ISNOx} \\
& s.t.\begin{cases}
\mathrm{P_{cyl}} = f(\alpha, r_1, h_1, r_2) \le 16.0 \\
t_r = f(\alpha, r_1, h_1, r_2) \le 720 \\
153 \le \alpha \le 159 \\
4.0 \le r_1 \le 6.0 \\
4.0 \le h \le 7.0 \\
20.5 \le r_2 \le 22.5
\end{cases}
\end{aligned} \tag{1}
$$

In Equation (1), ITE (%) represents the indicated thermal efficiency, $\mathrm{ISNO_x}$ (g/(kW·h)) represents the indicated specific NO_x emission, $\mathrm{P_{cyl}}$ (MPa) represents the peak in-cylinder pressure, and t_r (°C) represents the vortex front temperature. "Corner min" refers to the minimum value of the corresponding parameter in the optimized condition sample set, while "corner max" refers to the maximum value of the corresponding parameter in the optimized condition sample set.

The optimization process utilized NSGA-II, resulting in 30 different sets of Pareto optimal solutions. A population size of 100, a hybridization probability of 0.8, a variance probability of 0.05, a Pareto frontier factor of 0.3, and a genetic generation count of 1000 were employed as the optimal end conditions. To determine the best solution among the Pareto optimal solutions, this study evaluated the advantages and disadvantages of the 30 sets using the TOPSIS method, which is a widely used and effective approach for multi-objective decision analysis, providing a ranking based on the distance between superior and inferior solutions.

The 30 sets of Pareto optimal solutions were ranked using the TOPSIS method to identify the ideal optimal solutions and their corresponding combustion chamber structure parameters. The comparison of combustion chamber structure parameters before and after optimization is presented in Table 4.

Table 4. Comparison of combustion chamber structure parameters before and after optimization.

Item	Original Value	Optimal Value
Oil injection cone angle α (°)	156.0	157.2
Crater radius r_1 (mm)	5.0	4.2
Center depth h (mm)	5.5	5.0
Throat radius r_2 (mm)	21.5	22.2

Due to the limitations of the testing conditions, it was not feasible to physically test the optimized piston combustion chamber. To verify the accuracy of the simulation results, the optimization outcomes were further tested using 3D simulation CFD software.

Table 5 illustrates the comparison of the indicated thermal efficiency and the indicated specific NO_x emission with and without the optimized combustion chamber for the small agricultural diesel engines fueled with pure diesel (D100) and B20, respectively. When fueled with D100, the ITE increased by 0.63% and the $\mathrm{ISNO_x}$ emission increased by 1.55% with the optimized combustion chamber. When fueled with B20, the ITE remained almost the same as that with the unoptimized combustion chamber, while the $\mathrm{ISNO_x}$ emission reduced by 22.83% with the optimized combustion chamber. Compared to D100 with the unoptimized combustion chamber, the ITE only declined by 0.17% and the $\mathrm{ISNO_x}$ emission reduced by 8.28% with B20 fueling using the optimized combustion chamber. Compared to D100 fueling with the optimized combustion chamber, the ITE declined by 0.8% and the $\mathrm{ISNO_x}$ emission reduced by 9.97% with B20 fueling using the optimized combustion chamber. Thus, the optimized combustion chamber can ensure the power of small agricultural diesel engines using B20 biodiesel in highland environments without compromising the power output, while concurrently reducing NO_x emissions to a certain extent.

Table 5. Comparison of indicated thermal efficiency and indicated specific NO_x emission with and without the optimized combustion chamber.

Item	ITE (%)	ISNO$_x$ (g/(kW·h))
D100 without Opt	45.44	3.87
D100 with Opt	46.07	3.93
B20 without Opt	45.32	4.60
B20 with Opt	45.27	3.55

Figure 7 presents a comparison of the equivalence ratio, temperature, and NO_x generation of the diesel combustion chamber. From the figures, it is observed that the optimization of the combustion moment at 15 °CA results in a relatively higher equivalence ratio around the oil beam after injection, while the temperature is lower in the pit area and in the squeeze flow area compared to the original engine. This configuration makes it challenging to achieve an ideal condition for NO_x generation, leading to a partial reduction in combustion and a corresponding decrease in NO_x generation. Furthermore, as the crankshaft angle increases, NO_x is primarily generated in the crater area, and the optimized result exhibits lower NO_x generation in the bottom of the crater area compared to the original engine. In summary, the coordinated design of the combustion chamber structure and injection cone angle in the original diesel engine ensures engine power while effectively optimizing NO_x emissions.

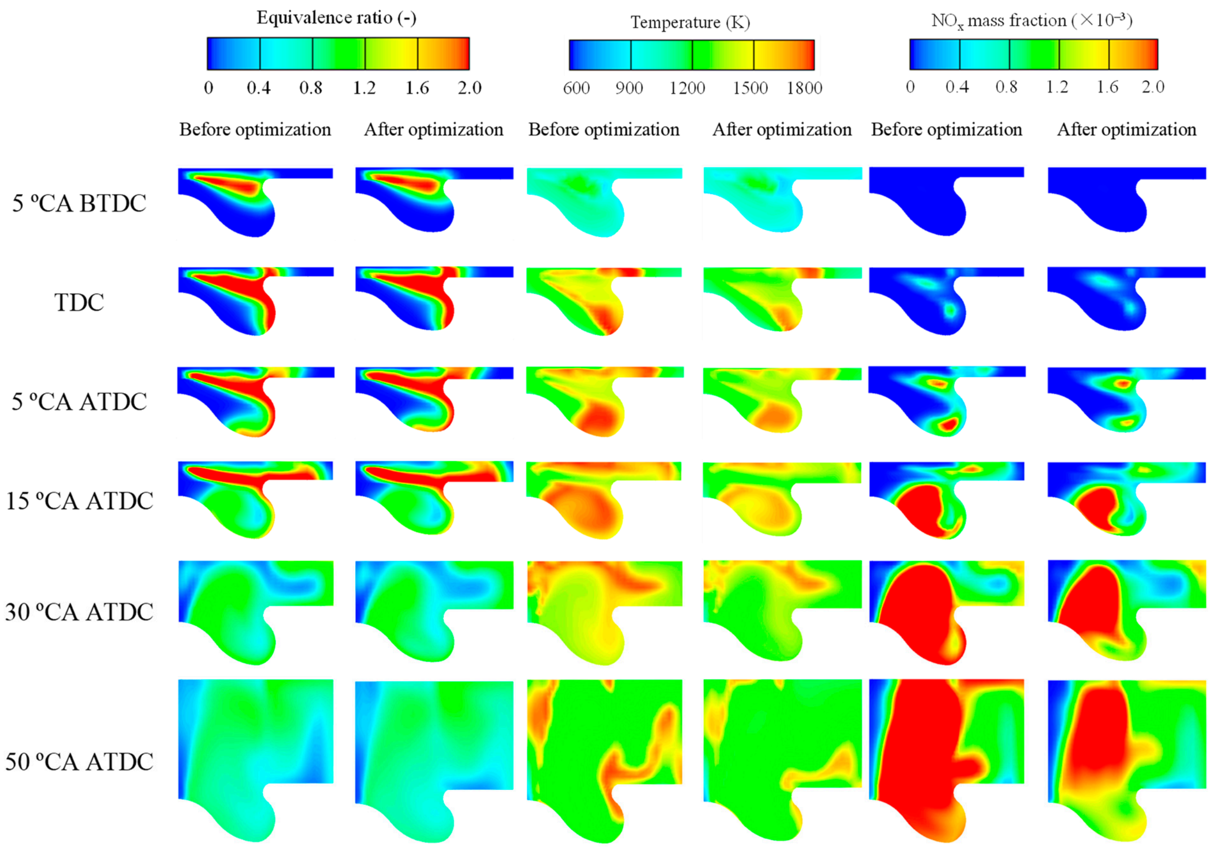

Figure 7. Distribution of equivalence ratio, in-cylinder temperature, and NO_x mass fraction before and after optimization.

4. Conclusions

To optimize NO_x emissions in a small agricultural diesel engine fueled with biodiesel in a plateau environment, a three-level four-factor full factorial design was used to conduct the experimental design, the BP neural network was used to predict the indicated thermal efficiency and the indicated specific NO_x emission, NSGA-II was employed to optimize the indicated thermal efficiency and the indicated specific NO_x emission, and the TOPSIS method was employed to filter out the ideal optimal solutions and their corresponding combustion chamber structure parameters and fuel injection parameters. Two main conclusions can be drawn from this study.

(1) Numerical modeling was conducted for small agricultural diesel engines in a plateau area, resulting in the establishment of a model capable of predicting the engine's operating conditions. The model exhibited a prediction accuracy of within 5% for the engine's combustion performance;

(2) For the working conditions of small agricultural diesel engines burning biodiesel in a plateau area, it was found feasible to utilize the full analysis factor design scheme and employ a BP neural network based on NSGA-II for multi-objective optimization. The optimization results demonstrated a 22.83% reduction in NO_x emissions compared to the original engine while maintaining the original engine's performance. This optimization successfully mitigates NO_x emissions while preserving engine performance.

Author Contributions: Conceptualization, Z.S. and J.W.; methodology, Z.S.; formal analysis, X.G.; investigation, X.G.; resources, J.W. and X.L.; data curation, J.W.; writing—original draft prepara-tion, Z.S.; writing—review and editing, J.W.; visualization, X.G.; supervision, X.L.; project administration, J.W. and X.L.; funding acquisition, J.W. and X.L. All authors have read and agreed to the published version of the manuscript.

Funding: This work was supported by the Yunnan Province Agricultural Joint Special Foundation (Grant No. 202101BD070001-110) and Yunnan Provincial Department of Education Scientific Research Fund Project (Grant No. 2022J0500).

Institutional Review Board Statement: Not applicable.

Informed Consent Statement: Not applicable.

Data Availability Statement: The data presented in this study are available on request from the corresponding author. The data are not publicly available due to the need for further research.

Conflicts of Interest: The authors declare no potential conflicts of interest with respect to research, authorship, and/or publication of this article.

References

1. Du, Y.; Fu, S.; Mao, E.; Zhu, Z.; Li, Z. Development situation and prospects of intelligent design for agricultural machinery. *Trans. Chin. Soc. Agric. Mach.* **2019**, *50*, 1–17.
2. Fu, M.; Ding, Y.; Yin, H.; Ji, Z.; Ge, Y.; Liang, B. Characteristics of agricultural tractors emissions under real-world operating cycle. *Trans. Chin. Soc. Agric. Eng.* **2013**, *29*, 42–48.
3. Tan, P.; Wang, D.; Lou, D.; Hu, Z. Progress of control technologies on exhaust emissions for agricultural machinery. *Trans. Chin. Soc. Agric. Eng.* **2018**, *34*, 1–14. [CrossRef]
4. Dahodwala, M.; Joshi, S.; Krishnamoorthy, H.; Koehler, E.W.; Franke, M. Evaluation of system configurations for downsizing a heavy-duty diesel engine for non-road applications. *SAE Int. J. Engines* **2016**, *9*, 2272–2285. [CrossRef]
5. Wang, J.; Shen, L.; Wen, Y.; Zhao, J. Effects of atmospheric pressure on combustion and emission of a small agricultural diesel engine at idle condition. *Trans. Chin. Soc. Agric. Eng.* **2020**, *36*, 73–79.
6. Ministry of Ecology and Environment of the People's Republic of China. *China Mobile Source Environmental Management Annual Report*; Ministry of Ecology and Environment of the People's Republic of China: Beijing, China, 2022.
7. Yu, L.; Ge, Y.; Tan, J.; He, C.; Wang, X.; Liu, H.; Zhao, W.; Guo, J.; Fu, G.; Feng, X.; et al. Experimental investigation of the impact of biodiesel on the combustion and emission characteristics of a heavy duty diesel engine at various altitudes. *Fuel* **2014**, *115*, 220–226. [CrossRef]
8. Liu, S.; Shen, L.; Bi, Y.; Lei, J. Effects of altitude and fuel oxygen content on the performance of a high pressure common rail diesel engine. *Fuel* **2014**, *118*, 243–249. [CrossRef]

9. Shen, L.; Yang, Y.; Lei, J.; Bi, Y.; Yan, W.; Tang, Y. Study of performance and emission of a turbocharged inter-cooling diesel engine at different altitudes. *Trans. CSICE* **2006**, *24*, 250–255.
10. Wang, X.; Yin, H.; Ge, Y.; Yu, L.; Xu, Z.; Yu, C.; Shi, X.; Liu, H. On-vehicle emission measurement of a light-duty diesel van at various speeds at high altitude. *Atmos. Environ.* **2013**, *81*, 263–269. [CrossRef]
11. Nadimi, E.; Przybyła, G.; Emberson, D.; Løvås, T.; Ziółkowski, Ł.; Adamczyk, W. Effects of using ammonia as a primary fuel on engine performance and emissions in an ammonia/biodiesel dual-fuel CI engine. *Int. J. Energy Res.* **2022**, *46*, 15347–15361.
12. Ma, Q.; Zhang, Q.; Liang, J.; Yang, C. The performance and emissions characteristics of diesel/biodiesel/alcohol blends in a diesel engine. *Energy Rep.* **2021**, *7*, 1016–1024. [CrossRef]
13. Mahmudul, H.M.; Hagos, F.Y.; Mamat, R.; Adam, A.A.; Ishak, W.F.W.; Alenezi, R. Production, characterization and performance of biodiesel as an alternative fuel in diesel engines—A review. *Renew. Sustain. Energy Rev.* **2017**, *72*, 497–509.
14. Suthisripok, T.; Semsamran, P. The impact of biodiesel B100 on a small agricultural diesel engine. *Tribol. Int.* **2018**, *128*, 397–409. [CrossRef]
15. Shen, Y.; Li, W.; Chen, G.; Zhang, W.; Chen, C.; He, K. Effects of biodiesel on the performance and emission characteristics of CI engine running at high altitude region. *Chin. Intern. Combust. Engine Eng.* **2015**, *36*, 150–156.
16. Si, P.; Chen, G.; Wang, X.; Mao, B.; Zheng, Z.; Yao, M. Effects of structure of combustion chamber and injector on heavy-duty diesel performance and emission characteristics. *Trans. Chin. Soc. Agric. Mach.* **2013**, *44*, 12–18.
17. Chen, H.; Wei, S.; Tang, D.; Li, C. Numerical simulation on the combustion and emission characteristics of a diesel engine with double ω combustion chamber. *Automot. Eng.* **2014**, *36*, 423–431.
18. Singh, P.; Tiwari, S.K.; Singh, R.; Kumar, N. Modification in combustion chamber geometry of CI engines for suitability of biodiesel: A review. *Renew. Sustain. Energy Rev.* **2017**, *79*, 101.
19. Lei, J.; Yu, Y.; Xian, Q.; Shen, L.; Song, G. Investigation and application of systematic design method for combustion chamber of diesel engine. *Trans. Chin. Soc. Agric. Eng.* **2020**, *36*, 36–46.
20. Taghavifar, H.; Khalilarya, S.; Jafarmadar, S. Engine structure modifications effect on the flow behavior, combustion, and performance characteristics of DI diesel engine. *Energy Convers. Manag.* **2014**, *85*, 20–32. [CrossRef]
21. Zheng, Z.; Wang, X.; Wang, H.; Zhu, Z.; Deng, Y. Optimization study on combustion chamber of a stoichiometric combustion natural gas engine. *Chin. Intern. Combust. Engine Eng.* **2020**, *41*, 1–8.
22. Guo, J.; Liu, Y.; Wu, B.; Su, W. Numerical simulation of piston bowl optimization for heavy-duty diesel engines with high charge density. *Chin. Intern. Combust. Engine Eng.* **2021**, *42*, 72–81.
23. Zhang, Y.; Du, H.; Sun, C. A study on optimization of diesel engine combustion chamber based on numerical simulation. *Chin. Intern. Combust. Engine Eng.* **2018**, *39*, 87–92.
24. Lee, J.; Jayun, C.; Dockoon, Y. A compression ratio selection method of the non-road diesel engine without EGR system to meet stage V emission standards. In Proceedings of the ASME 2017 Internal Combustion Engine Division Fall Technical Conference, Seattle, WA, USA, 15–18 October 2017; pp. 2017–3542.
25. Liu, M.; Yao, M.; Wang, H.; Zheng, Z.; Liang, H. Numerical simulation of combustion chamber optimization for thermal efficiency improvement of heavy-duty diesel engine. *J. Combust. Sci. Technol.* **2022**, *28*, 355–362.
26. Jaichandar, S.; Annamalai, K. Effects of open combustion chamber geometries on the performance of pongamia biodiesel in a DI diesel engine. *Fuel* **2012**, *98*, 272–279. [CrossRef]
27. Jaichandar, S.; Kumar, P.S.; Annamalai, K. Combined effect of injection timing and combustion chamber geometry on the performance of a biodiesel fueled diesel engine. *Energy* **2012**, *47*, 388–394. [CrossRef]
28. Jaichandar, S.; Annamalai, K. Combined impact of injection pressure and combustion chamber geometry on the performance of a biodiesel fueled diesel engine. *Energy* **2013**, *55*, 330–339. [CrossRef]
29. Li, J.; Yang, W.; An, H.; Maghbouli, A.; Chou, S. Effects of piston bowl geometry on combustion and emission characteristics of biodiesel fueled diesel engines. *Fuel* **2014**, *120*, 66–73. [CrossRef]
30. Premnath, S.; Devaradjane, G. Improving the performance and emission characteristics of a single cylinder diesel engine having reentrant combustion chamber using diesel and Jatropha methyl esters. *Ecotoxicol. Environ. Saf.* **2015**, *121*, 10–15. [CrossRef]
31. Bapu, B.R.R.; Saravanakumar, L.; Prasad, B.D. Effects of combustion chamber geometry on combustion characteristics of a DI diesel engine fueled with calophyllum inophyllum methyl ester. *J. Energy Inst.* **2017**, *90*, 82–100. [CrossRef]
32. Karthickeyan, V. Effect of combustion chamber bowl geometry modification on engine performance, combustion and emission characteristics of biodiesel fuelled diesel engine with its energy and exergy analysis. *Energy* **2019**, *176*, 830–852. [CrossRef]
33. Khan, S.; Panua, R.; Bose, P.K. The impact of combustion chamber configuration on combustion and emissions of a single cylinder diesel engine fuelled with soybean methyl ester blends with diesel. *Renew. Energy* **2019**, *143*, 335–351. [CrossRef]
34. Shivashimpi, M.M.; Alur, S.A.; Topannavar, S.N.; Dodamani, B.M. Combined effect of combustion chamber shapes and nozzle geometry on the performance and emission characteristics of CI engine operated on pongamia. *Energy* **2018**, *154*, 17–26. [CrossRef]
35. Rajashekhar, C.R.; Chandrashekar, T.K.; Umashankar, C.; Kumar, R.H. Studies on effects of combustion chamber geometry and injection pressure on biodiesel combustion. *Trans. Can. Soc. Mech. Eng.* **2012**, *36*, 429–438. [CrossRef]
36. Jia, G.; Tian, G.; Zhang, D. Effects of plateau environment on combustion and emission characteristics of a plateau high-pressure common-rail diesel engine with different blending ratios of biodiesel. *Energies* **2022**, *15*, 550. [CrossRef]

37. Jiao, Y.; Liu, R.; Zhang, Z.; Yang, C.; Zhou, G.; Dong, S.; Liu, W. Comparison of combustion and emission characteristics of a diesel engine fueled with diesel and methanol-Fischer-Tropsch diesel-biodiesel-diesel blends at various altitudes. *Fuel* **2019**, *243*, 52–59. [CrossRef]
38. Tan, Z.; Wang, J.; Chen, W.; Shen, L.; Bi, Y. Study on the influence of EGR on the combustion performance of biofuel diesel at different ambient simulated pressures. *Sustainability* **2021**, *13*, 7862. [CrossRef]
39. Hao, C.; Ge, Y.; Wang, X. Heavy-duty diesel engine fuel consumption comparison with diesel and biodiesel measured at different altitudes. *Int. J. Veh. Perform.* **2020**, *6*, 263–276. [CrossRef]
40. Li, X.; Zheng, Y.; Guan, C.; Cheung, C.S.; Huang, Z. Effect of biodiesel on PAH, OPAH, and NPAH emissions from a direct injection diesel engine. *Environ. Sci. Pollut. Res.* **2018**, *25*, 34131–34138. [CrossRef] [PubMed]
41. Hanjalić, K.; Popovac, M.; Hadžiabdić, M. A robust near-wall elliptic-relaxation eddy-viscosity turbulence model for CFD. *Int. J. Heat Fluid Flow* **2004**, *25*, 1047–1051. [CrossRef]
42. Dukowicz, J.K. *Quasi-Steady Droplet Phase Change in the Presence of Convection*; Los Alamos Scientific Laboratory: Los Alamos, NM, USA, 1979.
43. Liu, A.B.; Mather, D.; Reitz, R.D. Modeling the effects of drop drag and breakup on fuel sprays. *SAE Trans.* **1993**, *102*, 83–95.
44. Jiro, S.; Kobayashi, M.; Iwashita, S.; Fujimoto, H. Modeling of diesel spray impingement on a flat wall. *SAE Trans.* **1994**, *103*, 1918–1931.
45. Colin, O.; Benkenida, A. The 3-zones extended coherent flame model (ECFM3Z) for computing premixed/diffusion combustion. *Oil Gas Sci. Technol.* **2004**, *59*, 593–609. [CrossRef]
46. Komiyama, K.; Heywood, J.B. Predicting NOx emissions and effects of exhaust gas recirculation in spark-ignition engines. *SAE Transactions* **1973**, *82*, 1458–1476.
47. An, H.; Yang, W.; Maghbouli, A.; Li, J.; Chua, K. AA skeletal mechanism for biodiesel blend surrogates combustion. *Energy Convers. Manag.* **2014**, *81*, 51–59. [CrossRef]
48. Ambarish, D.; Samiddha, P.; Bijankumar, M. An experimental study on the performance and emission characteristics of a CI engine fueled with Jatropha biodiesel and its blends with diesel. *J. Mech. Sci. Technol.* **2014**, *28*, 1961–1966.